Desalination and Water Treatment
www.deswater.com

doi: 10.5004/dwt.2023.29467

291 (2023) 12–19
April

Preparation of high-performance PA/PDA-β-CD/PVDF composite loose nanofiltration membrane by β-cyclodextrin

Haoyang Zhang*, Ming Li, Honghai Yang, Jun Wang

College of Environmental Science and Engineering, Donghua University, 2999 North Renmin Road, Shanghai, China, Tel.: +86-21-677925396; emails: zhanghy9130@163.com (H. Zhang), 18217692535@163.com (M. Li), yhh@dhu.edu.cn (H. Yang), wangj@dhu.edu.cn (J. Wang)

Received 29 October 2022; Accepted 8 March 2023

ABSTRACT

The fractionation of dye and salt effectively is crucial in the nanofiltration of dyeing wastewater. However, the present commercial nanofiltration membrane often rejected dye and salt simultaneously due to the dense selective layer of the membrane. To obtain nanofiltration membranes with a loose selective layer, β-cyclodextrin (β-CD) was added to the co-deposition of dopamine/polyethyleneimine in the PA/PDA-β-CD/PVDF composite loose nanofiltration membrane by the method of combination of co-deposition and interfacial polymerization. The effect of β-CD content on the structure and morphologies of PA/PDA-β-CD/PVDF composite loose nanofiltration membrane was investigated. The chemical structure, microstructure, surface roughness, and hydrophilicity of the membrane surface were characterized by an infrared spectrometer (attenuated total reflection-Fourier-transform infrared spectroscopy), scanning electron microscope, atomic force microscope, and dynamic water contact angle meter. The filtration performance of the PA/PDA-β-CD/PVDF composite loose nanofiltration membrane was tested by filtration experiments. The results showed that with the increase of β-CD concentration, the hydrophilicity, water flux, and salt permeability of the selective layer were significantly increased, indicating that β-CD had improved the porosity and hydrophilicity of the selective layer. When the β-CD concentration was 2 g/L, the flux of water and dyeing wastewater was the maximum, but the dye rejection was lower than 90%. The performance of the composite nanofiltration membrane with the β-CD concentration of 1 g/L was the best.

Keywords: Polyvinylidene fluoride; β-cyclodextrin; Loose nanofiltration membrane; Dyeing wastewater

1. Introduction

Dye wastewater is not only a large quantity but also highly toxic and difficult to degrade, which seriously threatens the environment and human health [1–3]. In recent years, more and more attention has been paid to the application of nanofiltration membranes in dye wastewater treatment. However, the present commercial nanofiltration membrane intercepts the salt and dye simultaneously in the dyeing wastewater treatment because of its high density. The presence of salt in the dyeing wastewater affects the reuse of the dye or the subsequent degradation of the dye. To effectively separate the salt from the dye in the dyeing wastewater, the researchers prepared loose nanofiltration membranes by adjusting the selective layer structure of the composite nanofiltration membrane which makes the salt permeate while intercepting the dye. Presently, the preparation of loose nanofiltration membranes reported in the literature was mainly by adding some nanoparticles or their modified substances in the co-deposition stage of composite nanofiltration membranes prepared by the method of combination of co-deposition and interface polymerization to improve the porosity of the selected layer [4]. For

* Corresponding author.

example, inorganic nanoparticles such as TiO_2, SiO_2, and CeO_2 were added to the co-deposition of dopamine (DA)/polyethyleneimine (PEI) or other systems of co-deposition to improve the porosity of the selected layer [5–9], but inorganic nanoparticles have problems of aggregation and poor compatibility with organic matter. To improve the dispersion uniformity of inorganic nanoparticles and the compatibility with organic matter, researchers modified inorganic nanoparticles [10], for example, modified SiO_2 by carboxylation [11] and ethanol-modified $FeNiO_4$ nanoparticles [12], carboxylated TiO_2/calcium alginate hydrogel [13], etc. In addition to inorganic nanoparticles and their modified substances, some organic nanoparticles [14–17], such as adding UIO-66-NH_2 active substances [18], carboxymethyl chitosan-zinc oxide biological nanocomposite materials to improve the selection layer [19]. Metal-organic skeleton (MOF) [20,21], HKUST-1 [22], and so on, were added too. However, there were few studies on the effects of β-cyclodextrin (β-CD) on the porosity of the selective layer till now.

Cyclodextrin is a hollow truncated cone with a molecular size of about 1–2 nm. The hollow structure of cyclodextrin plays a significant role in forming water channels on the membrane surface [23–25]. Wu et al. [26] added cyclodextrin as an additive to membranes and prepared novel β-cyclodextrin (β-CD)/mylar nanofiltration composite membranes by in situ interface polymerization in the presence of β-CD using benzoyl chloride (TMC) and triethanolamine (TEOA) as raw materials. However, there has been no report on how to improve the porosity and hydrophilicity of PA/PDA/PVDF composite nanofiltration membrane by adding β-CD in the DA/PEI co-deposition stage.

Some researchers have prepared nanofiltration membranes using β-cyclodextrin. Wu et al. [26] prepared nanofiltration membranes by interfacial polymerization using TEOA and β-CD as aqueous substances and TMC as oil-phase substances. The flux of the membrane is 61 ($L/m^2 \cdot h$) under the working pressure of 0.6 MPa, and the retention rate of Na_2SO_4 is 23%. The high working pressure is not conducive to energy saving. Xue et al. [27] prepared a high-throughput β-CD/GQDs nanofiltration membrane by interfacial polymerization using β-cyclodextrin (β-CD) as water monomer, graphene quantum dots (GQDs) as an additive and tri formyl chloride (TMC) as the organic monomer. The preparation method is complicated and the conditions are harsh, so it is difficult to prepare a nanofiltration membrane easily. Glycerol, as a polyhydroxy substance, is also modified on the surface of the membrane by glycerol, which has a significant effect on improving the permeability of the membrane [28] and has reference significance for the preparation of nanofiltration membrane by using β-CD. Wang et al. [29] prepared an antifouling loose nanofiltration membrane for the effective separation of dyes and salts by constructing a porous cyclodextrin polymer layer on the membrane substrate. Octoclonic cyclodextrin macromonomer with vertical chain vinyl can be prepared by the method of controlled free radical polymerization and esterification, and used for membrane production. On the other hand, thin-film composite reverse osmosis membrane can be tuned for the desired performance by surface modification owing to the top polyamide layer, which can be modified [30–32].

In this paper, the PA/PDA-β-CD/PVDF composite loose nanofiltration membrane was prepared by the method of combination of co-deposition and interfacial polymerization. β-cyclodextrin (β-CD) was added to the co-deposition of DA/PEI to improve the porosity of the selective layer of PA/PDA-β-CD/PVDF composite loose nanofiltration membrane. The chemical structure, microstructure, surface roughness, and hydrophilicity of the selected layer were characterized by infrared spectroscopy attenuated total reflection-Fourier-transform infrared spectroscopy (ATR-FTIR), scanning electron microscopy (SEM), atomic force microscopy (AFM), and dynamic water contact angle analyzer. The filtration performance of PA/PDA-β-CD/PVDF composite loose nanofiltration membrane was tested by filtration experiment, and the effect of β-CD content on the structure and performance of PA/PDA-β-CD/PVDF composite loose nanofiltration membrane was discussed. The operation stability of the membrane in the treatment of simulated Reactive Black 5 (RB5) dyeing wastewater was also discussed.

2. Experimental set-up

2.1. Materials

Polyvinylidene fluoride (PVDF, FR904, Shanghai Organic Fluorine Material Co., Ltd., Shanghai, China); analytically pure, Sinopharm Chemical Reagent Co., Ltd., China); benzoyl chloride (TMC, 98%, Shanghai Maclean Co., Ltd., Shanghai, China); tris-HCl buffer solution (pH = 8.5, Shanghai Naicheng Biological Co., Ltd., Shanghai, China); copper sulfate pentahydrate ($CuSO_4 \cdot 5H_2O$, 99%), hydrogen peroxide (H_2O_2, 30%), N,N-dimethylacetamide (DMAc), dopamine hydrochloride (DA, 98%), polyethyleneimine (PEI, MW1800), polyvinylpyrrolidone (PVP K30), polyethylene glycol (PEG, MW800), Reactive Black 5 (RB5) sodium chloride (NaCl, superior grade pure) and *n*-hexane (analytically pure) all come from the Sinopharm Chemical Reagent Co., Ltd., (China) β-cyclodextrin (β-CD, 98%, Rhawn Reagent).

2.2. Equipment

MSC cup type ultrafilter (300 mL, Mosu Scientific Equipment Co., Ltd.); Conductivity meter (DS-11A, Shanghai Laiqi Instrument Co., Ltd., China); field-emission scanning electron microscope (S-4800, Carl Zeiss, Germany); atomic force microscopy (Agilent-S5500, Agilent Technologies); UV-visible spectrophotometer (UV-7504PC, Shimadzu Company, Japan); Fourier-transform infrared spectrometer (NEXUS-670, BURKE, Germany); contact angle meter (SL200KS, KINO Industry Co., Ltd.).

2.3. Fabrication of composite NF membranes

Preparation of substrate membranes: PVDF (18%wt), PVP K30(4%wt), and DMAc (78%wt) were placed in a 250 mL conical flask, stirred in the water bath at 90°C till a transparent PVDF casting solution was obtained, then defoamed. The defoamed casting solution was slowly poured onto a dry clean glass plate and scraped into a film of about 0.2 mm thickness using a glass rod. The nascent film was immediately put into a water bath at 35°C for phase separation. After the film is completely cured and formed

into a membrane, take it out and immerse in deionized water for more than 24 h to remove the solvent [33].

Fabrication of PVDF loose nanofiltration membranes: (1) preparation of co-deposition system. DA (2 g/L) was dissolved in tris buffer solution (pH = 8.5, 10 mL), firstly. Then $CuSO_4 \cdot 5H_2O$ (0.024 g) and H_2O_2 (40 μL), PEI aqueous solution (10 mL, 2 g/L) and β-cyclodextrin (β-CD) (0, 0.5, 1, 1.5, and 2 g/L) were added successively and being stirred to obtain a transparent solution. (2) Co-deposition process: the substrate membrane was fixed on the bottom of the container only the upside can contact the co-deposition system. After being deposited for 60 min, the membrane was taken out, rinsed with deionized water several times, and dried at 35°C in a constant temperature oven [34]. (3) Interfacial polymerization process: The deposited membrane was fixed on the bottom of the container after being dried, the deposited surface was upside, then 0.2%wt. TMC *n*-hexane solution was poured onto the deposited surface to cross-link for 5 min, then, the solution on the membrane surface was poured out. After that, the membrane was rinsed with an appropriate amount of *n*-hexane to remove the unreacted TMC. then was kept in the constant temperature oven for 5 min at 50°C. Finally, the membrane was washed with deionized water and immersed in deionized water to be used.

2.4. Characterization of membrane

2.4.1. Chemical structure

The surface chemical structure of the nanofiltration membrane was analyzed by ATR-FTIR. The infrared spectrogram obtained from material analysis reflects the types of functional groups contained in the material, and the structure of the compound can be determined by analyzing the characteristic spectrum and fingerprint region. The infrared spectra of DA, PEI, β-CD, and PVDF were measured by the potassium bromide tablet method. Firstly, the potassium bromide dried in the oven was ground into powder in the mortar, and then the samples to be tested were added to fully ground, and the samples were pressed to be used for the measurement of the infrared spectrum. The chemical structure of PA/PDA-β-CD/PVDF composite loose nanofiltration membrane selective layer was qualitatively analyzed by the ATR method. The prepared samples were cut into square samples and measured by Fourier-transform infrared spectrometer.

2.4.2. Microstructure surface roughness of the PA/PDA-β-CD/PVDF loose nanofiltration membrane

The PA/PDA-β-CD/PVDF loose nanofiltration membrane was cut into a 2 cm × 2 cm square. And The microstructure of the surface and cross-section of PA/PDA-β-CD/PVDF loose nanofiltration membrane was observed by a field emission scanning electron microscope (S-4800). The surface roughness of the PA/PDA-β-CD/PVDF loose nanofiltration membrane was characterized by atomic force microscopy (Agilent-s5500).

2.4.3. Surface hydrophilicity

The hydrophilicity of the selective layer of the composite nanofiltration membrane was characterized by the water contact angle on the surface of the selective layer. If the water contact angle was less than 90°, the membrane surface was hydrophilic, and the smaller the contact angle, the better the hydrophilicity. If the contact angle is greater than 90°, the membrane surface is hydrophobic. The water contact angles of the PA/PDA-β-CD/PVDF composite loose nanofiltration membrane selective layer supplemented with β-cyclodextrin were measured by a full-automatic contact angle analyzer (Kino SL200KS). The results were fitted by Young–Laplace.

2.5. Characterization of filtration performance

2.5.1. Pure water flux test

Cut the membrane into a suitable circular shape and fix it in the ultrafiltration cup. The pure water flux of the composite nanofiltration membrane was measured at 0.1 MPa after being preloaded for 30 min at 0.15 MPa, the filtrate volume was recorded every 10 min within 1 h. The pure water flux was calculated by Eq. (1) as follows:

$$J_w = \frac{V}{A \cdot t \cdot p} \tag{1}$$

where J_w is pure water flux, L/m²·h·bar; V is filtrate volume, *L*; *A* is the effective area of the membrane, 36.6 × 10^{-4} m²; *t* is the time required to obtain *V* volume filtrate, *h*; *p* is the operating pressure, 1 bar.

2.5.2. Molecular weight cut-off (MWCO) of the PVDF loose nanofiltration membranes

The MWCO was characterized by PEG solution (1 g/L). The PEG rejection was calculated by Eq. (2) as follows:

$$R_1 = \frac{C_p - C_f}{C_p} \times 100\% \tag{2}$$

where R_1 is PEG800 rejection, %; C_p and C_f were the PEG solution concentration before and after filtrating, mg/L, respectively, which were characterized by the total organic carbon (TOC) of the PEG solution.

2.6. Application in the treatment of simulating RB5 dyeing wastewater and the investigation of operational stability

2.6.1. Simulating RB5 dyeing wastewater flux and the dye rejection

The concentration of RB5 and NaCl was 0.1 and 0.5 g/L, respectively in the simulating dyeing wastewater. The filtration process was the same as that of pure water. The dyeing wastewater flux was calculated by Eq. (1), too. The RB5 rejection was calculated by Eq. (3) as follows:

$$R_2 = \frac{C_0 - C}{C_0} \times 100\% \tag{3}$$

where R_2 is dye rejection, %; C_0 and *C* were the RB5 concentration before and after filtration, respectively, which

were characterized by UV-7504PC UV-visible spectrophotometer at 593 nm wavelength.

The salt rejection was calculated by Eq. (3), too. However, the salt concentration in the simulated dyeing wastewater was characterized by the electrical conductivity meter.

2.6.2. Investigation of operational stability

The operational stability of PA/PDA-β-CD/PVDF loose nanofiltration membrane in the treatment of simulating RB5 dyeing wastewater was investigated within the time of 6 h. The filtrate volume was recorded every 0.5 h.

3. Results and discussion

3.1. Surface chemical structure of composite nanofiltration membrane

The chemical structure of the PA/PDA-β-CD/PVDF loose nanofiltration membrane was qualitatively analyzed by ATR-FTIR. The results are shown in Fig. 1.

From Fig. 1 it can be found that the characteristic peaks of DA and PEI appear between 3,200 and 3,500 cm^{-1}, which belong to amino peaks. The characteristic peak of PVDF is located at 1,000–1,400 cm^{-1}, which belongs to the absorption vibration of the C–F bond. In the PA/PDA-β-CD/PVDF composite loose nanofiltration membrane without β-cyclodextrin, the characteristic peak of DA appeared at 3,395 cm^{-1}. In the spectrogram of PA/PDA-β-CD/PVDF composite loose nanofiltration membrane, the characteristic peak of β-cyclodextrin appeared at 3,347 and 1,042 cm^{-1}. However, the spectra of PA/PDA/PVDF composite nanofiltration membrane without β-cyclodextrin did not show these two peaks, indicating that β-cyclodextrin has been fixed on the surface of the composite nanofiltration membrane by co-deposition of DA. The characteristic peak of C=O appears in 1,690–1,740 cm^{-1}; The characteristic peak of C=C resonance vibration in the aromatic ring appears at 1,540–1,695 cm^{-1}. The characteristic peak of C=N tensile vibration appears in 1,650–1,680 cm^{-1}. At the same time, the C=O carbonyl absorption peak appears at 1,724 cm^{-1}. Compared with PA/PDA-β-CD/PVDF composite loose nanofiltration membrane without β-cyclodextrin, the absorption peak of the carbonyl group in the loose polyester network formed by the crosslinking of β-cyclodextrin and TMC was increased. The occurrence of this peak is consistent with the study of Xue et al. [35]. The absorption peaks due to C=C resonance vibration and C=N tensile vibration in the aromatic ring appear at 1,651 cm^{-1}, and the characteristic peak of PEI at 2,929 cm^{-1} disappears in the composite nanofiltration membrane, indicating that polyamide (PA) is generated on the surface of PA/PDA-β-CD/PVDF composite loose nanofiltration membrane.

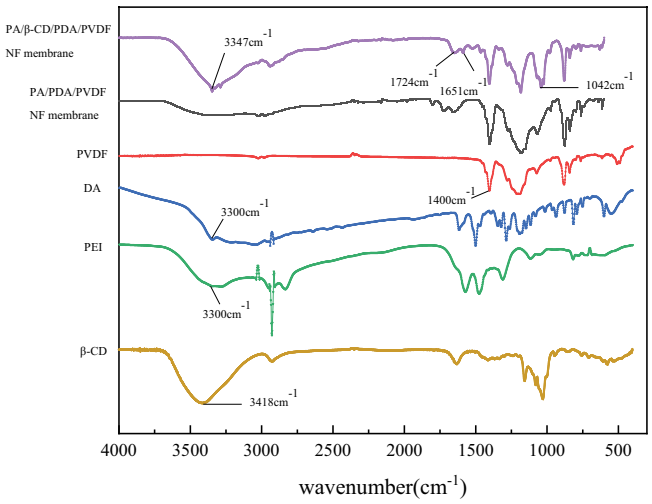

Fig. 1. Infrared spectra of β-cyclodextrin, dopamine, polyethyleneimine, polyvinylidene fluoride and composite nanofiltration membranes (ATR-FTIR).

3.2. Effect of β-CD concentration on the microstructure of the selective layer

The microstructure and surface roughness of PA/PDA-β-CD/PVDF composite loose nanofiltration membrane was characterized by SEM and AFM images which are displayed in Fig. 2. It can be seen from Fig. 2a–c that when the content of β-CD was 0 g/L, the surface of PA/PDA-β-CD/PVDF composite loose nanofiltration membrane selection layer is relatively flat, and there are fewer nodules and holes on the selection layer. With the content of β-CD up to 1 g/L, relatively dense nodules appeared on the surface of the membrane. The reason is that β-cyclodextrin crosslinked with TMC based on the PA selection layer to form a loose polyester cross-linking network, which is helpful to increase the effective surface area of the film, thus increasing the flux of the film. This phenomenon is more significant when the content of β-CD increased to 2 g/L, the size of nodules increased further, and the roughness of the membrane significantly improved too. The cross-section electron microscopy showed that the thickness of the selective layer of the composite nanofiltration membrane increased with the increase of the content of β-CD, but the inner layer of the selective layer became more loose, leading to the increase in the flux.

3.3. Surface hydrophilicity of the loose nanofiltration membrane

The hydrophilicity of PA/PDA-β-CD/PVDF composite loose nanofiltration membrane with β-cyclodextrin was characterized by the water contact angle on the membrane surface. The variation of surface water contact angle of the PA/PDA-β-CD/PVDF loose nanofiltration membrane with β-CD concentration is shown in Fig. 3.

It can be seen from Fig. 3 that the water contact angle gradually decreased with the increase of β-CD concentration. The water contact angle decreased from 52.98° to 32.88° with the β-CD concentration increased from 0 to 2 g/L, which means that the hydrophilicity of the PVDF loose nanofiltration membranes was enhanced highly with the increase of the β-CD concentration. The reason is that β-CD is an external hydrophilic and inner cavity hydrophobic substance with a large amount of hydrophilic hydroxy groups which leads to the increase of the surface hydrophilicity of the PVDF loose nanofiltration membranes. So, the surface water contact angle decreased with the increase of β-CD.

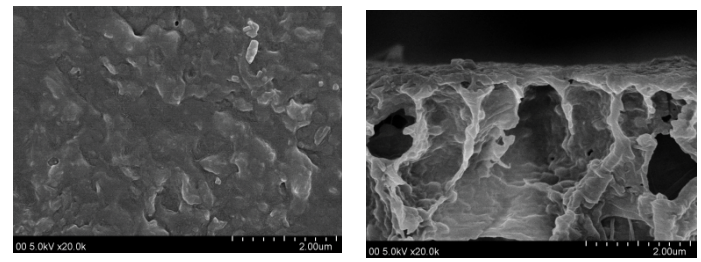

(a)β-CD 0 g/L Ra=13.9 nm Rq=17.3 nm

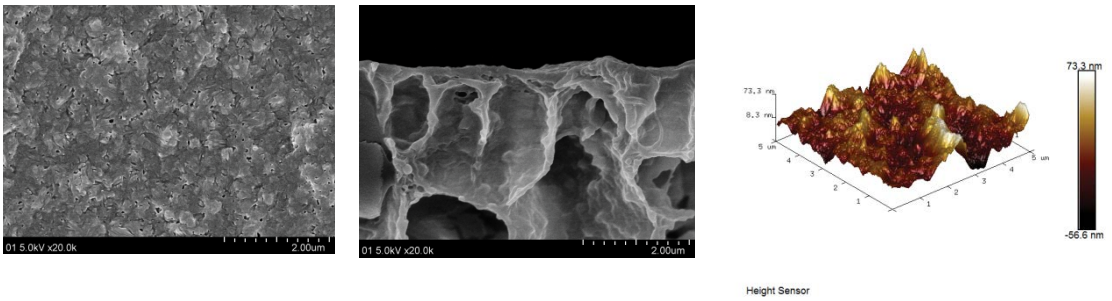

(b)β-CD 1 g/L Ra=12.1 nm Rq=16.1 nm

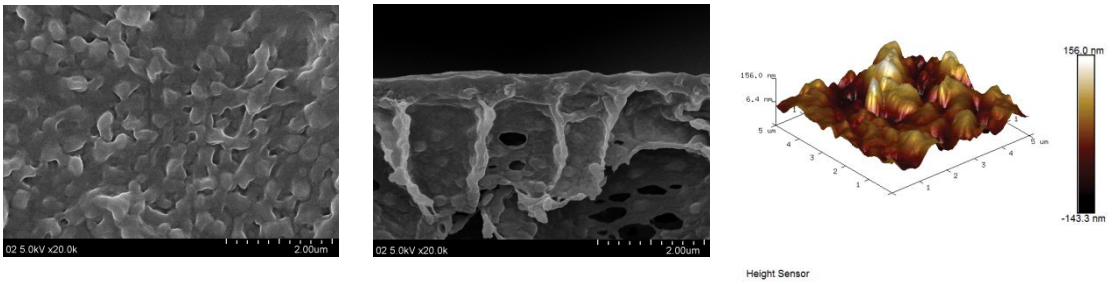

(c)β-CD 2 g/L Ra=34.0 nm Rq=43.2 nm

Fig. 2. (a–c) Effect of β-cyclodextrin concentration on the microstructure of selective layer of PA/PDA-β-CD/PVDF composite loose nanofiltration membrane.

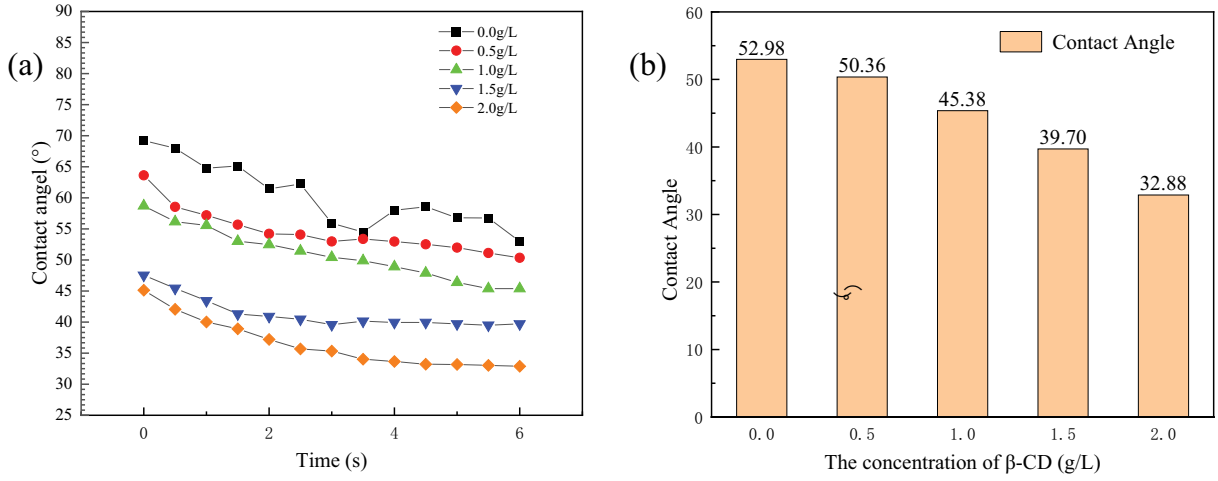

Fig. 3. Effects of β-cyclodextrin concentration on the surface water contact angle (a) dynamic surface water contact angle and (b) static surface water contact angle.

3.4. Effect of β-CD concentration on the pure water flux and PEG800 rejection

Fig. 4a and b show the effect of β-CD on pure water flux and PEG800 rejection of PA/PDA-β-CD/PVDF loose nanofiltration membrane.

As shown in Fig. 4, with the concentration of β-CD increasing from 0 to 2 g/L, the pure water flux increased from 7.0 to 15.2 L/(m²·h) gradually. This is because β-CD not only enhanced the hydrophilicity greatly of the PA/PDA-β-CD/PVDF composite loose nanofiltration membrane but also made the selective layer loose which was due to the large amount of molecular of β-CD. In addition, the surface of PA/PDA-β-CD/PVDF composite loose nanofiltration membrane became rougher with the increase of β-CD which resulted in the effective filtration area of the membrane increase. However, the PEG800 rejection decreased from 99.9% to 58.2% with the increase of β-CD from 0 to 2 g/L. The PEG800 rejection decreased to below 90% when the content of β-CD was 1.5 and 2.0 g/L, respectively. The reason was that the selective layer became too loose which led to the PEG800 rejection decrease with the content of β-CD increasing to above 1.5 g/L. This means that when the content of β-CD was greater than 1.5 g/L, the MWCT of PA/PDA-β-CD/PVDF composite loose nanofiltration membrane was greater than PEG800. Namely, the PA/PDA-β-CD/PVDF composite loose nanofiltration membrane maybe not reject the dye with the molecular was about 800 Da or less than 800 Da effectively when the content of β-CD was greater than 1.5 g/L.

3.5. Application in the treatment of simulated dyeing wastewater and the operational stability

3.5.1. Effect of β-cyclodextrin content on the dyeing wastewater flux and RB5 rejection

Fig. 5 shows the variation of dyeing wastewater flux, dye, and salt rejection of PA/PDA-β-CD/PVDF composite loose nanofiltration membrane with the change of β-CD content in the treatment of simulating RB5 dyeing wastewater.

As shown in Fig. 5, the simulated dyeing wastewater flux increased from 6.56 to 14.75 L/(m²·h) with the increase of β-CD from 0 to 2 g/L. The variation tendency was similar to that of pure water flux. The RB5 rejection and salt rejection both tended to decline with the increase of β-CD. The above variations were due to the structure of the selective layer becoming looser with the increase of β-CD. The RB5 rejection was below 90% when the content of β-CD was up to 1.5 g/L. So, the optimal content of β-CD is 1 g/L if the RB5 rejection must be greater than 90%. And the simulating RB5 dyeing wastewater flux was much better when the content of β-CD was 1 g/L.

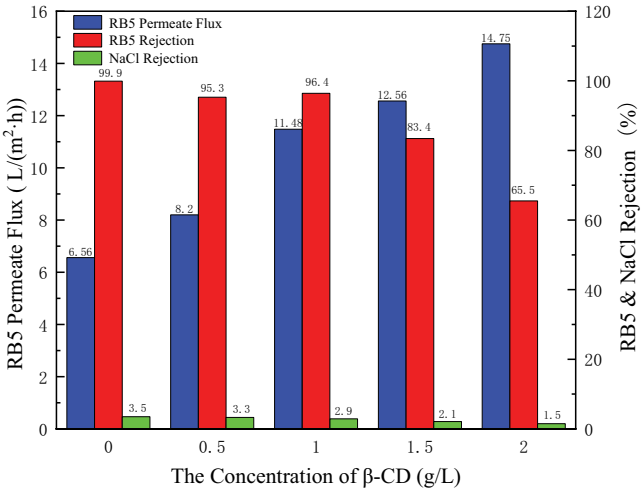

Fig. 5. Effects of β-cyclodextrin addition on the flux of simulated dye wastewater and the rejection of dye and salt by PA/PDA-β-CD/PVDF composite loose nanofiltration membrane.

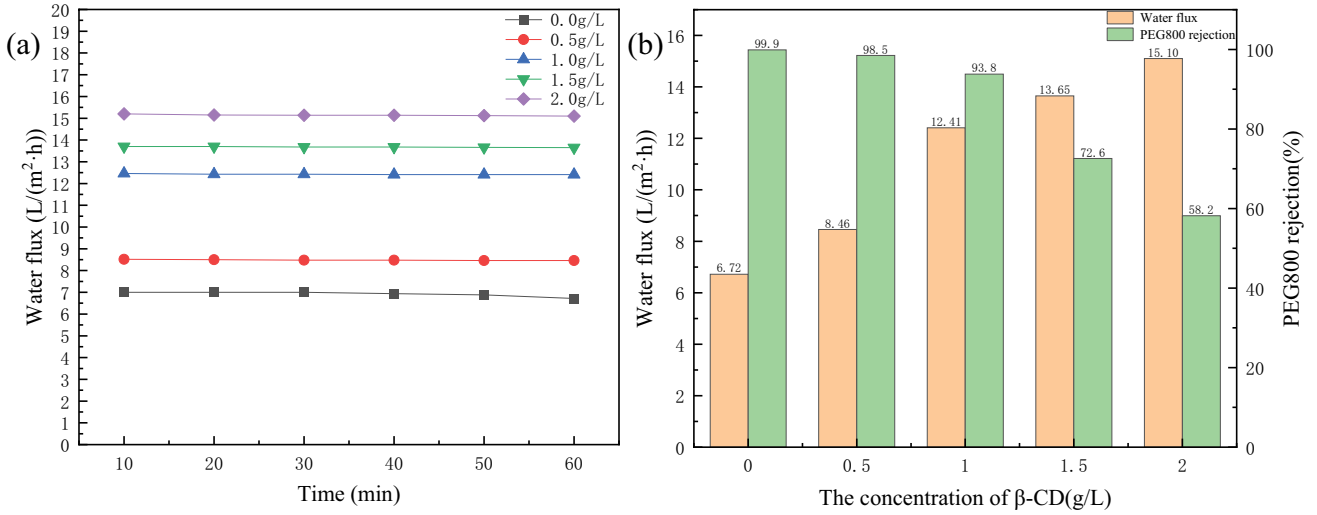

Fig. 4. (a) Effect of β-cyclodextrin addition on pure water flux of PA/PDA-β-CD/PVDF composite loose nanofiltration membrane and (b) effect of β-cyclodextrin addition on PEG800 rejection.

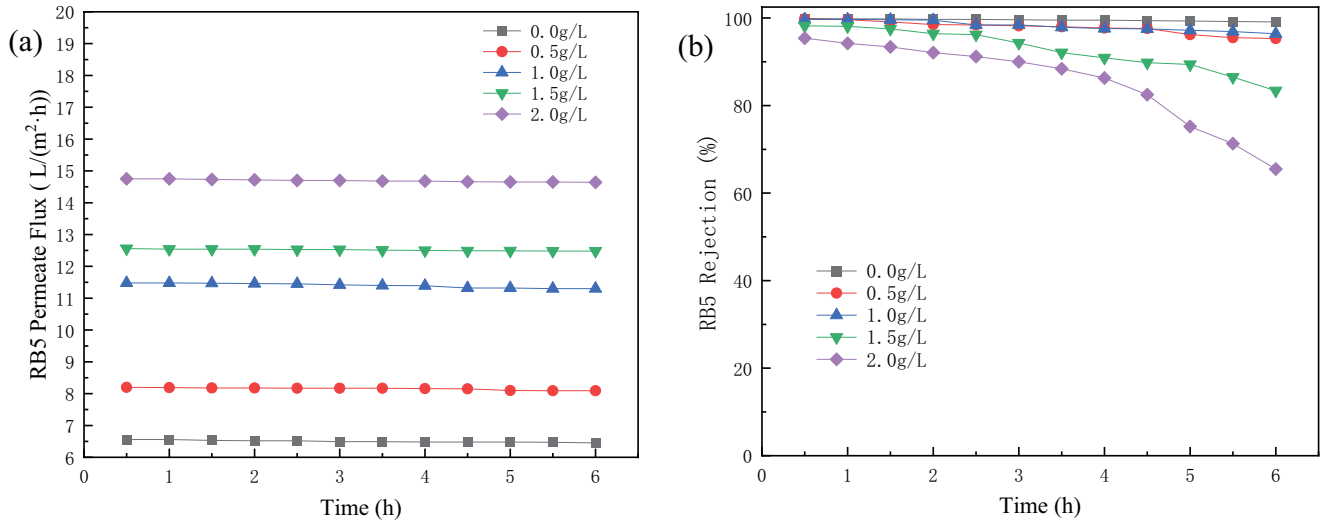

Fig. 6. Results of the operational stability of the PA/PDA-β-CD/PVDF loose nanofiltration membrane in the simulating RB5 dyeing wastewater treatment: (a) the variation of the simulating RB5 dyeing wastewater flux with time and β-cyclodextrin and (b) the change of RB5 rejection with time and β-cyclodextrin.

3.5.2. Operational stability of the PA/PDA-β-CD/PVDF loose nanofiltration membrane

Fig. 6a and b show the operational stability of the PA/PDA-β-CD/PVDF loose nanofiltration membrane in the treatment of the simulating RB5 dyeing wastewater.

It can be seen from Fig. 6 that with the content of β-CD in the range of 0 to 1.0 g/L, the PA/PDA-β-CD/PVDF loose nanofiltration membrane could keep significant operational stability, and the RB5 rejection had remained above 95%. However, when the content of β-CD was 1.5 and 2 g/L, the RB5 rejection decreased to 83.4% and 65.5%, respectively. This is because the integrity of the selective layer was destroyed due to the selective layer becoming too loose with the content of β-CD increasing to 1.5 g/L.

4. Conclusion

The above results stated that with the increase of β-CD content, a loose polyester layer appears in the selective layer on the surface of the composite nanofiltration membrane. The roughness and porosity of the membrane surface are increased, the hydrophilicity was enhanced, and the flux of pure water and dye wastewater gradually increased. The optimal β-D content is 1 g/L, which made the PA/PDA-β-CD/PVDF loose nanofiltration membrane obtain better flux, RB5 rejection, and operational stability in the simulating RB5 wastewater treatment. Under the optimum conditions, the RB5 rejection and the salt rejection were 99.7% and 2.9%, which realized the better separation of dye/salt.

References

[1] G. Xue, Technology progress of dyeing wastewater treatment, Ind. Water Treat., 41 (2021) 10–17.
[2] J. Jiang, X. He, X. Xiong, X. Zhang, H. Ren, Research progress on toxicity characteristics and control technologies of textile dyeing wastewater, Ind. Water Treat., 41 (2021)77–87.
[3] G. Zhao, J. Sun, Y. Zhang, H. Wang, J. Wu, Research progress of advanced oxidation technology in treatment of printing and dyeing wastewater, Appl. Chem. Ind., 50 (2021) 2550–2554,2558.
[4] R. Zhang, Y. Su, X. Zhao, Y. Li, J. Zhao, Z. Jiang, A novel positively charged composite nanofiltration membrane prepared by bio-inspired adhesion of polydopamine and surface grafting of poly(ethylene imine), J. Membr. Sci., 470 (2014) 9–17.
[5] H. Mahdavi, N. Mazinani, A.A. Heidari, Poly(vinylidene fluoride) (PVDF)/PVDF-g-polyvinylpyrrolidone (PVP)/TiO_2 mixed matrix nanofiltration membranes: preparation and characterization, Polym. Int., 69 (2020) 1187–1195.
[6] M. Zargar, Y. Hartanto, B. Jin, S. Dai, Polyethylenimine modified silica nanoparticles enhance interfacial interactions and desalination performance of thin film nanocomposite membranes, J. Membr. Sci., 541 (2017) 19–28.
[7] P. Mobarakabad, A.R. Moghadassi, S.M. Hosseini, Fabrication and characterization of poly(phenylene ether-ether sulfone) based nanofiltration membranes modified by titanium dioxide nanoparticles for water desalination, Desalination, 365 (2015) 227–233.
[8] J.L. Wang, X.L. Gao, J. Wang, Y. Wei, Z.K. Li, C.J. Gao, O-(carboxymethyl)-chitosan nanofiltration membrane surface functionalized with graphene oxide nanosheets for enhanced desalting properties, ACS Appl. Mater. Interfaces, 7 (2015) 4381–4389.
[9] T. Tavangar, M. Karimi, M. Rezakazemi, K.R. Reddy, T.M. Aminabhavi, Textile waste, dyes/inorganic salts separation of cerium oxide-loaded loose nanofiltration polyethersulfone membranes, Chem. Eng. J., 385 (2020) 123787, doi: 10.1016/j.cej.2019.123787.
[10] C. Li, J. Li, W.H. Zhang, N.X. Wang, S.L. Ji, Q.F. An, Enhanced permeance for PDMS organic solvent nanofiltration membranes using modified mesoporous silica nanoparticles, J. Membr. Sci., 612 (2020) 118257, doi: 10.1016/j.memsci.2020.118257.
[11] X.Z. Wei, X.F. Xu, J.W. Wu, C.X. Li, J.Y. Chen, B.S. Lv, B.K. Zhu, H. Xiang, SiO_2-modified nanocomposite nanofiltration membranes with high flux and acid resistance, J. Appl. Polym. Sci., 136 (2019) 47436, doi: 10.1002/app.47436.
[12] S. Ansari, A.R. Moghadassi, S.M. Hosseini, Fabrication of novel poly(phenylene ether ether sulfone) based nanocomposite membrane modified by Fe_2NiO_4 nanoparticles and ethanol as organic modifier, Desalination, 357 (2015) 189–196.
[13] X.L. Wang, W. Qin, L.X. Wang, K.Y. Zhao, H.C. Wang, H.Y. Liu, J.F. Wei, Desalination of dye utilizing carboxylated TiO_2/calcium alginate hydrogel nanofiltration membrane with

high salt permeation, Sep. Purif. Technol., 253 (2020) 117475, doi: 10.1016/j.seppur.2020.117475.
[14] V. Vatanpour, H. Karimi, S.I. Ghazanlou, Y. Mansourpanah, M.R. Ganjali, A. Badiei, E. Pourbashir, M.R. Saeb, Anti-fouling polyethersulfone nanofiltration membranes aided by amine-functionalized boron nitride nanosheets with improved separation performance, J. Environ. Chem. Eng., 8 (2020) 104454, doi: 10.1016/j.jece.2020.104454.
[15] L.L. Huang, Z.Y. Li, Y. Luo, N. Zhang, W.X. Qi, E. Jiang, J.J. Bao, X.P. Zhang, W.J. Zheng, B.G. An, G.H. He, Low-pressure loose GO composite membrane intercalated by CNT for effective dye/salt separation, Sep. Purif. Technol., 256 (2021) 117839, doi: 10.1016/j.seppur.2020.117839.
[16] H. Siddique, L.G. Peeva, K. Stoikos, G. Pasparakis, M. Vamvakaki, A.G. Livingston, Membranes for organic solvent nanofiltration based on preassembled nanoparticles, Ind. Eng. Chem. Res., 52 (2013) 1109–1121.
[17] Z. Rahimi, A.A. Zinatizadeh, S. Zinadini, M.C.M. van Loosdrecht, β-cyclodextrin functionalized MWCNTs as a promising antifouling agent in fabrication of composite nanofiltration membranes, Sep. Purif. Technol., 247 (2020) 116979, doi: 10.1016/j.seppur.2020.116979.
[18] Y.Q. Gong, S.J. Gao, Y.Y. Tian, Y.Z. Zhu, W.X. Fang, Z.G. Wang, J. Jin, Thin-film nanocomposite nanofiltration membrane with an ultrathin polyamide/UIO-66-NH_2 active layer for high-performance desalination, J. Membr. Sci., 600 (2020) 117874, doi: 10.1016/j.memsci.2020.117874.
[19] K. Ekambaram, M. Doraisamy, Surface modification of PVDF nanofiltration membrane using carboxymethylchitosan-zinc oxide bionanocomposite for the removal of inorganic salts and humic acid, Colloid. Surf., A, 525 (2017) 49–63.
[20] J. Campbell, R.P. Davies, D.C. Braddock, A.G. Livingston, Improving the permeance of hybrid polymer/metal-organic framework (MOF) membranes for organic solvent nanofiltration (OSN) – development of MOF thin films via interfacial synthesis, J. Mater. Chem., A, 3 (2015) 9668–9674.
[21] Y.P. Bao, Y.F. Chen, T.T. Lim, R. Wang, X. Hu, A novel metal–organic framework (MOF)–mediated interfacial polymerization for direct deposition of polyamide layer on ceramic substrates for nanofiltration, Adv. Mater. Interfaces, 6 (2019) 1900132, doi: 10.1002/admi.201900132.
[22] X.Y. Guo, D.H. Liu, T.T. Han, H.L. Huang, Q.Y. Yang, C.L. Zhong, Preparation of thin film nanocomposite membranes with surface modified MOF for high flux organic solvent nanofiltration, AlChE J., 63 (2017) 1303–1312.
[23] L.F. Villalobos, T.F. Huang, K.-V. Peinemann, Cyclodextrin films with fast solvent transport and shape-selective permeability, Adv. Mater., 29 (2017) 1606641, doi: 10.1002/adma.201606641.
[24] A.L. Taka, K. Pillay, X.Y. Mbianda, Nanosponge cyclodextrin polyurethanes and their modification with nanomaterials for the removal of pollutants from wastewater: a review, Carbohydr. Polym., 159 (2017) 94–107.
[25] Y.J. Tang, B.J. Shen, B.Q. Huang, Z.M. Zhan, Z.L. Xu, High permselectivity thin-film composite nanofiltration membranes with 3D microstructure fabricated by incorporation of β-cyclodextrin, Sep. Purif. Technol., 227 (2019) 115718, doi: 10.1016/j.seppur.2019.115718.
[26] H.Q. Wu, B.B. Tang, P.Y. Wu, Preparation and characterization of anti-fouling β-cyclodextrin/polyester thin film nanofiltration composite membrane, J. Membr. Sci., 428 (2013) 301–308.
[27] J. Xue, J. Shen, R. Zhang, F. Wang, S. Liang, X. You, Q. Yu, Y. Hao, Y. Su, Z. Jiang, High-flux nanofiltration membranes prepared with β-cyclodextrin and graphene quantum dots, J. Membr. Sci., 612 (2020) 118465, doi: 10.1016/j.memsci.2020.118465.
[28] H.D. Raval, M.D. Samnani, M.V. Gauswami, Surface modification of thin film composite reverse osmosis membrane by glycerol assisted oxidation with sodium hypochlorite, Appl. Surf. Sci., 427 (2018) 37–44.
[29] Y. Wang, C. Bao, D. Li, J. Chen, X. Xu, S. Wen, Z. Guan, Q. Zhang, Y. Ding, Y. Xin, Y. Zou, Antifouling and chlorine-resistant cyclodextrin loose nanofiltration membrane for high-efficiency fractionation of dyes and salts, J. Membr. Sci., 661 (2022) 120925, doi: 10.1016/j.memsci.2022.120925.
[30] H.D. Raval, J.J. Trivedi, S.V. Joshi, C.V. Demurari, Flux enhancement of thin film composite RO membrane by controlled chlorine treatment, Desalination, 250 (2010) 945–949.
[31] D. Ankoliya, B. Mehta, H. Raval, Advances in surface modification techniques of reverse osmosis membrane over the years, Sep. Sci. Technol., 54 (2019) 293–310.
[32] A.R. Kavaiya, H.D. Raval, Highly selective and antifouling reverse osmosis membrane by crosslinkers induced surface modification, Environ. Technol., 43 (2022) 2155–2166.
[33] Z. Jiang, R. Tao, J. Wang, Structure, properties and application of PA/Anthraquinone/PVDF composite nanofiltration membrane, Chin. J. Environ. Eng., 16 (2022) 1218–1226.
[34] H. Cui, Z. Li, J. Wang, Preparation of PA/PDA/PVDF composite nanofiltration membrane and its application in simulated RB5 dye wastewater treatment, New Chem. Mater., 50 (2022) 153–160,165.
[35] J. Xue, Z.W. Jiao, R. Bi, R.N. Zhang, X.D. You, F. Wang, L.J. Zhou, Y.L. Su, Z.Y. Jiang, Chlorine-resistant polyester thin film composite nanofiltration membranes prepared with β-cyclodextrin, J. Membr. Sci., 584 (2019) 282–289.